

# Efficiency of Different Roof Vent Designs on Natural Ventilation of Single-Span Plastic Greenhouse

Adnan Rasheed<sup>1</sup>, Jong Won Lee<sup>2</sup>, Hyeon Tae Kim<sup>5</sup>, and Hyun Woo Lee<sup>1,3,4\*</sup>

<sup>1</sup>Department of Agricultural Engineering, Kyungpook National University, Daegu 702-701, Korea

<sup>2</sup>Department of Horticulture Environment System, Korea National College of Agriculture and Fisheries, 1515, Kongjwipatjwi-ro, Deokjin-gu, Jeonju-si, Jeollabuk-do 54874, Republic of Korea

<sup>3</sup>Institute of Agricultural Science & Technology, Kyungpook National University, Daegu 702-701, Korea

<sup>4</sup>Smart Agriculture Innovation Center, Kyungpook National University, Daegu 41566, Korea

<sup>5</sup>Department of Bio-Industrial Machinery Engineering., GyeongsangNational University. (Institute of Agricultural and Life Sciences), Jinju 660-701, Korea

**Abstract.** In the summer season, natural ventilation is commonly used to reduce the inside air temperature of greenhouse when it rises above the optimal level. The greenhouse shape, vent design, and position play a critical role in the effectiveness of natural ventilation. In this study, computational fluid dynamics (CFD) was employed to investigate the effect of different roof vent designs along with side vents on the buoyancy-driven natural ventilation. The boussinesq hypothesis was used to simulate the buoyancy effect to the whole computational domain. RNG K-epsilon turbulence model was utilized, and a discrete ordinates (DO) radiation model was used with solar ray tracing to simulate the effect of solar radiation. The CFD model was validated using the experimentally obtained greenhouse internal temperature, and the experimental and computed results agreed well. Furthermore, this model was adopted to compare the internal greenhouse air temperature and ventilation rate for seven different roof vent designs. The results revealed that the inside-to-outside air temperature differences of the greenhouse varied from 3.2 to 9.6°C depending on the different studied roof vent types. Moreover, the ventilation rate was within the range from 0.33 to 0.49 min<sup>-1</sup>. Our findings show that the conical type roof ventilation has minimum inside-to-outside air temperature difference of 3.2°C and a maximum ventilation rate of 0.49 min<sup>-1</sup>.

**Additional key words :** air flow, CFD, greenhouse cooling, greenhouse thermal environment

## Introduction

The light, humidity, carbon dioxide concentration, temperature, and ventilation rate are the key factors influencing the greenhouse micro-environment (Pontikakos et al., 2006). Natural ventilation is a primary method to control humidity, temperature, and carbon dioxide concentration inside greenhouses (Lee and Short, 2000). Natural ventilation is the most effective among passive cooling techniques in lowering high air temperatures inside greenhouses. In the summer season, when the air temperature inside the greenhouse rises above the optimal level, natural ventilation is commonly used to reduce it. Agricultural greenhouses are predominantly naturally ventilated to control the inside air temperature at a reduced energy cost (Rasheed et al., 2018).

The size, position, and shape of vents are the crucial to the effectiveness of natural ventilation design. To design and optimize natural ventilation systems, it is important to conduct both qualitative and quantitative analysis of natural ventilation (López et al., 2011). In the past, many studies investigated greenhouse natural ventilation experimentally and numerically. The CFD tool provides a cost-effective way of design and optimization in agri-food industry. CFD has been applied in studies on crop farming, including greenhouses (Bartzanas et al., 2013). CFD is a valuable tool for investigations of the natural ventilation of buildings (Bartzanas et al., 2004) that has enabled research on the complex airflow patterns and conducting thermal analysis (Hong et al., 2017). CFD techniques have been applied in some studies to explore the effects exerted by different factors operating in greenhouses on natural ventilation, which is discussed below.

\*Corresponding author: whlee@knu.ac.kr

Received June 30, 2019; Revised July 22, 2019;

Accepted July 23, 2019

Mistriotis et al. (1997) used a CFD tool to examine the effect of the greenhouse length on the ventilation rate. The studies conducted by Lee and Short (2000); Haxaire et al. (2000), and Campen and Bot (2003) evaluated the influence of wind speed, wind direction, and vent opening on the natural ventilation rate of a greenhouse by using a CFD technique. Lee and Short (2001) did study on verification of CFD simulation of wind speed and temperature distribution inside the multi-span greenhouse. Additionally, many studies investigated the impact of the side and roof vent openings and the direction and speed of the wind on the greenhouse ventilation rate. Kacira et al. (2004b) investigated the effects different greenhouse vents configurations on natural ventilation rate of a two-span greenhouse. This study further studied the ventilation efficiency of a greenhouse while using a combination of side and roof vents. Interestingly, Shklyar and Arbel (2004) used a CFD code to explore the air flow pattern in a pitched-roof single-span greenhouse. In addition, Bartzanas et al. (2004) studied the effect of different configurations of tunnel greenhouse vents on the temperature pattern and airflow inside the tunnel. Pontikakos et al. (2006) use CDF tool to studied the natural ventilation efficiency inside the two-span greenhouse. Fatnassi et al. (2006) studied the effect of air flow greenhouse thermal environment of multi-span greenhouse in the presence of an insect screen; different roof and side vents arrangements were investigated. Kacira et al. (2004a) and Bournet et al. (2007) conducted numerical studies to assess the effect of different windward and leeward vents arrangements on the natural ventilation rate of a multi-span greenhouse. Moreover, Baeza et al. (2009) studied the effect of greenhouse side vents opposing distance on the buoyancy-driven natural ventilation in a multi-span greenhouse. Tong et al. (2009) used the CFD numerical simulation of investigate the temperature distribution inside the Chinese solar greenhouse. Jung-Soo et al. (2014) did a wind tunnel test to verify the CFD modeling and to improve the accuracy of the CFD code for the analysis of airflow inside the greenhouse. Benni et al. (2016) studied the different vent configuration of multi-span greenhouse aiming to identify the optimal configuration of greenhouse summer cooling. Lee et al. (2018) conducted research

on the wind-driven natural ventilation rate inside a single-span greenhouse by using a CFD code, taking into account the following parameters: wind speed and direction, different greenhouse shapes, and vent openings. Recently, Senhaji et al. (2019) performed a CFD study using different side and roof vents configurations with the same wind speed directions to investigate the mass air flow rate and temperature distribution inside the multi-chapels greenhouse.

In this research, we used ANSYS Fluent, a CFD tool, to study the effect of different roof vents designs combined with side vents on the inside thermal environment of a single-span greenhouse. Here, we considered the buoyancy-driven natural ventilation effect exerted on the greenhouse internal air temperature and ventilation rate, in the absence of the wind or at an exceedingly low wind speed. The effectiveness of the reduction in the greenhouse internal air temperature and ventilation rate of all the selected roof vent designs commonly used for greenhouse natural ventilation were investigated. The present research was conducted to develop an improved naturally efficient greenhouse design.

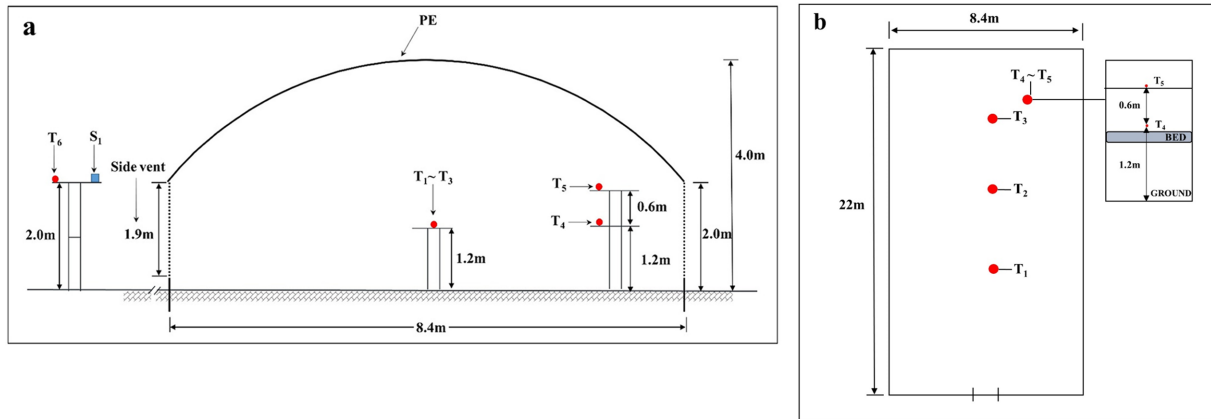
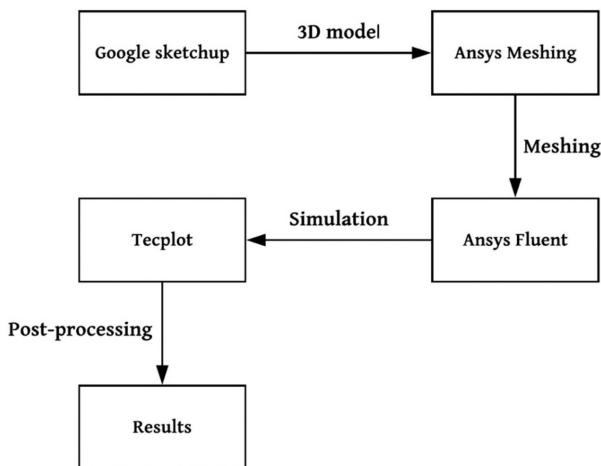
## Materials and Methods

### 1. Experimental greenhouse

The experimental greenhouse was a rectangular-based, round-roofed, east-west oriented, single-span greenhouse covered with a 0.15 mm thick polyethylene (PE) film, located at Daegu (latitude 35.53°N, longitude 128.36°E, elevation 48m), South Korea. The dimensions of the greenhouse were 22m × 8.4m × 4m, with a total floor area of 184.8m<sup>2</sup>, and roof curvature angle of 25.5°. The outside weather data recorded were as follow: solar radiation, wind speed, wind direction angle, and outside air temperature were, 962w·m<sup>-2</sup>, 1.5m·s<sup>-1</sup>, 110°, 28°C, respectively. Moreover, the weather parameters were recorded around the solar midday of July. The outside weather data was collected to use as an input in CFD model and greenhouse internal air temperature were measured for the validation of the CFD results. The characteristics of the weather data are presented in Table 1. The air temperature inside the greenhouse was measured at five different locations, three sensors were placed at the center line along the length of the greenhouse, and two sensors were mounted at one side

**Table 1.** Characteristics of the weather data used in the simulations.

Weather parameter	Unit	Time interval	Sensor	Data recorded
Temperature	°C	10 min	TR-76Ui-H, TECPEL	Field recorded
Solar radiation	kW	10 min	CMP3, Kipp & Zonen	Field recorded
Wind speed	ms <sup>-1</sup>	10 min	JY-WS161B, Jingang	KMA
Wind direction	degree	10 min	JY-WS161B, Jingang	KMA


**Fig. 1.** Dimensions and sensor position of the experimental greenhouse (a) vertical (b) horizontal view.

**Fig. 2.** Flow chart of the procedure.

of the greenhouse at different elevations, the air temperature sensors positions and dimensions of the experimental greenhouse are illustrated in Fig. 1. The measured air temperature was utilized for comparison with the numerical modeling results for validation. During the experimental period, there was no crop inside the greenhouse, and it was naturally ventilated by continuously opened side vents only.

## 2. CFD modeling

A computational fluid dynamics (CFD) program, (V.18.2, Fluent, ANSYS - FluentInc) was employed to predict the natural ventilation effect on the greenhouse internal air temperature and ventilation rate for various greenhouse and roof vent designs combined with side vents. The flow chart of the whole process is presented in Fig. 2. For this study, the first step pre-processing was conducted using Google SketchUp™ pro ver. 2015 software to prepare 3D models of greenhouses. Further, meshing was carried out in the ANSYS mesh component. In the second step, simulations were run for multiple cases using ANSYS Fluent ver. 18.2. Finally, post-processing of the simulation results was implemented by (Tecplot 360 2017 R2) software.

## 3. Computational domain and boundary conditions

The program used the finite method to numerically solve the Navier-Stokes equations, i.e., the mass, energy, and the momentum balances, permitting the calculation of the air velocity and the temperature. The Boussinque hypothesis was adopted to simulate the buoyancy effect to the whole computational

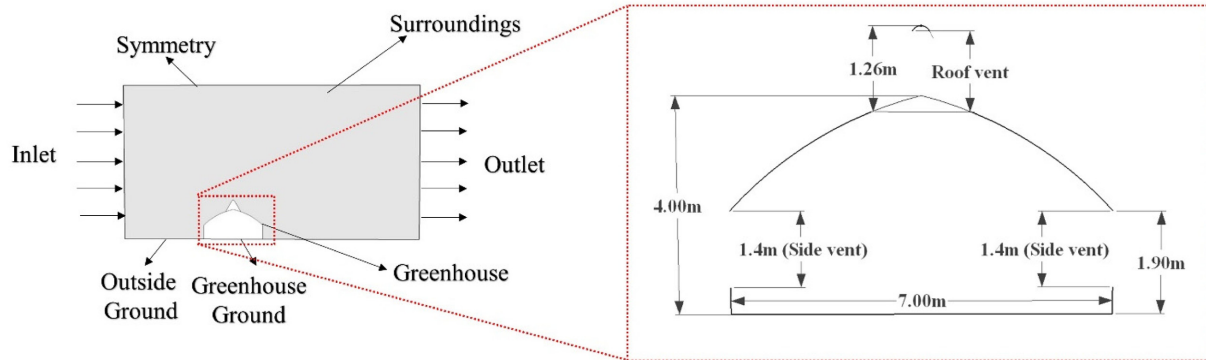


Fig. 3. Schematic diagram of computational domain and dimensions of the gothic-shaped conical roof vent greenhouse.

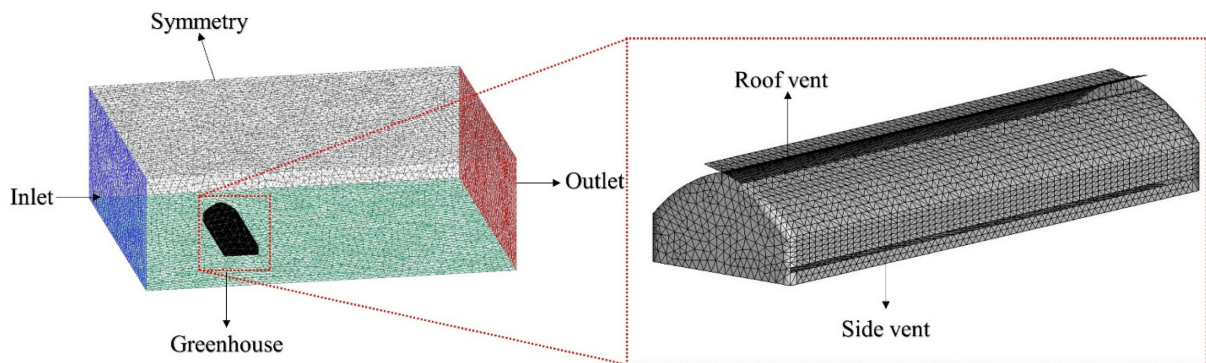


Fig. 4. Sketch showing rectangular computational domain and greenhouse structure meshing.

domain. We studied buoyancy-driven natural ventilation to establish the effect of greenhouse vents on the inside air temperature under the worst-case scenario. RNG K-epsilon turbulence model was employed, which has been previously used in many studies for this type of analysis (Baeza et al., 2009). The discrete ordinates (DO) radiation model was used with solar ray tracing to simulate the effect of solar radiation. The Fig. 3 depicts the computational domain and dimensions of the gothic-shaped conical roof vent greenhouse, and Fig. 4 illustrates the meshing of the rectangular computation domain and the greenhouse. The details of the meshing are listed in Table 2, and Table 3 represents the data of the boundary conditions and material properties used in the simulations. Fig. 5 shows the configuration of the studied roof vents designs along with side vents. Table 4 shows the detail of the greenhouse shapes, side and roof vent sizes and shapes of all studied cases.

Table 2. Mesh properties.

Properties	Value
Type of mesh	Hybrid
Number of meshes	1.5 million
Size function	Curvature
Curvature normal angle	10°
Element size	0.001m
Relevance	25

Table 3. Boundary conditions and material properties.

Parameter	Unit	Value
Direct Solar radiation	$W \cdot m^{-2}$	1500
Beam solar radiation	$W \cdot m^{-2}$	200
Wind velocity	$m \cdot s^{-1}$	0
Outside temperature	K	300
<b>Outside air properties</b>		
Temperature	K	300
Specific heat	$J \cdot kg^{-1} \cdot K^{-1}$	1006.43
Density	$kg \cdot m^{-3}$	1.225
Thermal conductivity	$W \cdot m^{-1} \cdot K^{-1}$	0.0242
Viscosity	$kg \cdot m^{-1} \cdot s^{-1}$	1.7894e-05

Table 3. Continued.

Greenhouse soil properties		
Thermal conductivity	$W \cdot m^{-1} \cdot K^{-1}$	1.89
Specific heat	$J \cdot kg^{-1} \cdot K^{-1}$	1500
Density	$kg \cdot m^{-3}$	2000
PE cover properties		
Thermal conductivity	$W \cdot m^{-1} \cdot K^{-1}$	0.33
Specific heat	$J \cdot kg^{-1} \cdot K^{-1}$	2300
Density	$kg \cdot m^{-3}$	923
Optical properties of PE		
Transmittance	-	0.91
Absorptivity	-	0.01

## Results and Discussion

To validate the CFD model, the experimentally recorded greenhouse internal air temperatures at different points were compared with the CFD predicted air temperature, the results of which are presented in Table 5. The CFD computed results obtained using conditions identical to those of the experimental greenhouse. The computed results had a good agreement with the ones obtained in the experiment. The computed values at locations  $T_1$ ,  $T_2$ ,  $T_3$ , and  $T_4$ , exhibited a small air temperature difference from the experimentally obtained ones,

Table 4. Details of the studied cases (different side and roof vents opening sizes).

Case	Shape	Side vent size	Roof vent size/shape
Case 1	Gothic	Closed	Closed
Case 2	Gothic	1.4	Roll-up vent on eave
Case 3	Gothic	1.4	Roll-up vent on ridge
Case 4	Round	1.4	Chimneys
Case 5	Gothic	1.4	0.5
Case 6	Even-roof	1.4	0.5
Case 7	Gothic	1.4	Conical type
Case 8	Gothic	1.4	Gambrel type

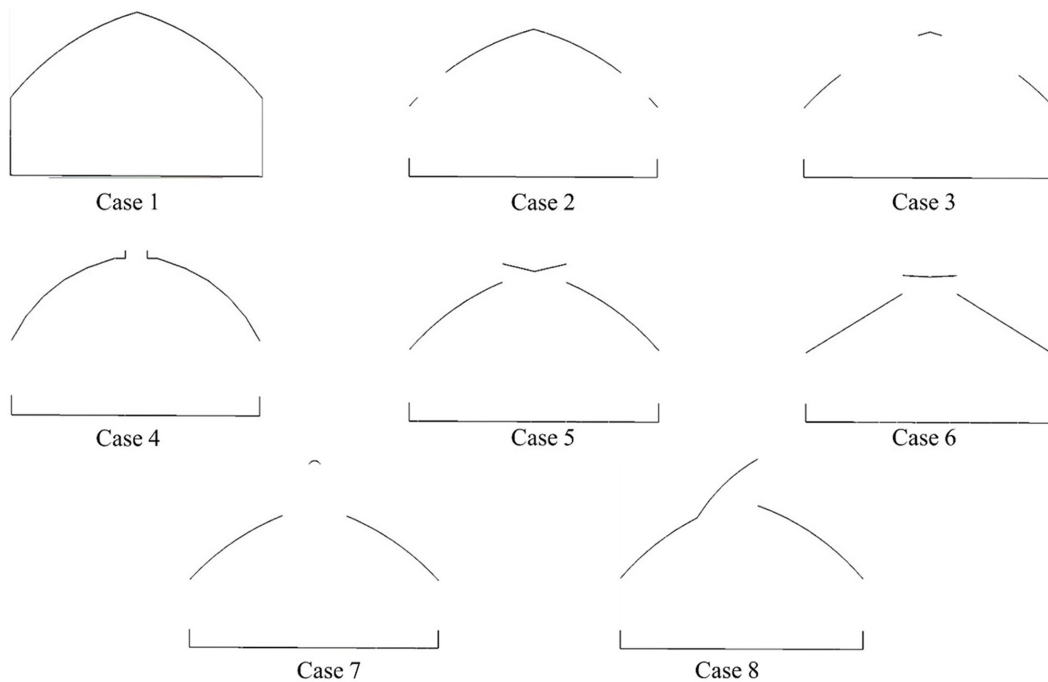


Fig. 5. Configurations of the studied cases.

**Table 5.** Validation results.

Sensor	Shape	Temp (°C)
T <sub>1</sub>	Experiment	34.4
	Simulated	35.5
T <sub>2</sub>	Experiment	34.5
	Simulated	34.5
T <sub>3</sub>	Experiment	35
	Simulated	34.5
T <sub>4</sub>	Experiment	35.5
	Simulated	34.5
T <sub>5</sub>	Experiment	35
	Simulated	33.8

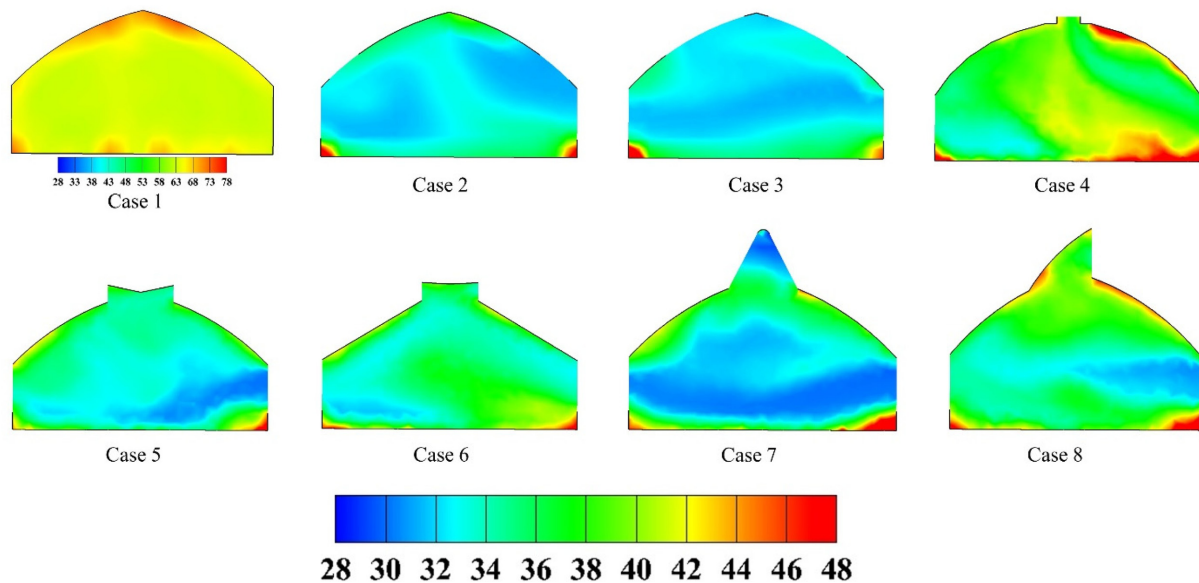
which was less than 1°C, for location T<sub>5</sub>, the difference was 1.2°C.

Fig. 6 illustrates the air temperature contours of all selected cases of different greenhouse roof ventilation systems. Simulations were carried out to establish the best roof ventilation system combined with the side vents of the single-span greenhouse. The reduction in greenhouse internal air temperature was compared with reference to a fully closed greenhouse. The air temperature value was measured at five different points along the width of the greenhouse at the height of 1.2 meter from the ground level and comparison was made between average air temperature inside the greenhouse.

**Table 6.** Inside air temperature of the greenhouse at 1.2 m height for all cases.

Case	Air temperature (°C)
Case 1	61.75
Case 2	31.55
Case 3	30.85
Case 4	36.45
Case 5	31.75
Case 6	34.95
Case 7	30.05
Case 8	32.55

The results showed that case 7 had the lowest air temperature than the other cases, as can be observed in Table 6. Moreover, as can be seen, the air flow was from the side to the roof vents because, due to the extremely low wind conditions, the air moved from the bottom to up caused by the gravity force. In Fig. 7, the contour is presented of the wind speed inside the gothic-shaped greenhouse with continuous side and roof-vent openings. To observe the buoyancy-driven natural ventilation, the wind speed inside the greenhouse was measured when the outside wind speed was 0m·s<sup>-1</sup>. As can be seen from the results, the wind speed was slightly higher at both side vents (inlet) and roof vent (outlet). The air entered from both side vents and exited from the roof vents causing a reduction in



**Fig. 6.** Contours of the inside air temperature (°C) of the greenhouses with different roof vent systems.

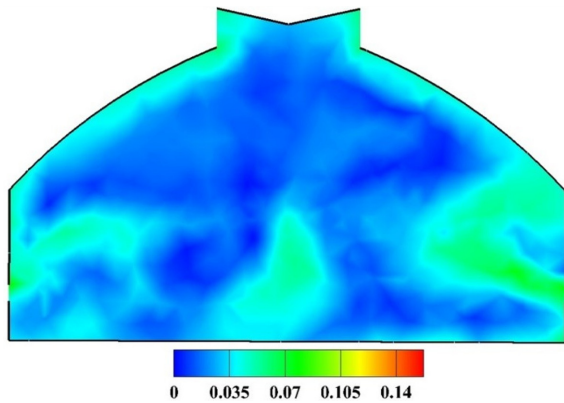


Fig. 7. Contour of the wind speed ( $\text{m}\cdot\text{s}^{-1}$ ) inside the greenhouse.

the greenhouse air temperature.

For better understanding, the results are presented and compared in Fig. 8 with respect to the inside-to-outside air temperature difference and air exchange rate of all the studied cases. It can be seen that case seven gothic-shaped (conical type vent) had a low inside-to-outside air temperature difference of  $3.2^\circ\text{C}$  and a high air exchange rate of  $0.49\text{min}^{-1}$ , higher exchange rate causes low air temperature differences. As it can be seen from the results that higher the air exchange rate results in lower the inside-to-outside air temperature difference. The descending order of air exchange rate for all cases was as follow; 7, 3, 6, 2, 5, and 8. Furthermore, these results revealed that case 6 had a higher air exchange rate than cases 2, 5, 8, and 4, but the inside-to-outside air temperature difference was higher than the ones in these cases because of even-roofed shape of the greenhouse, which leads to reaching a higher air temperature due to reception u more solar energy inside the greenhouse.

Further analysis was performed using the gothic-shaped conical type roof vent greenhouse with different commonly used natural ventilation configurations which included: only roof-vent opening, only side-vent opening, and combined side and roof-vent openings. The results are illustrated in Fig. 9, in which the comparison can be seen of the internal air temperature of the greenhouse at a height of 1.2 m with different vent opening configurations. Our results revealed that, in the case of only side-vent opening, and combined vents opening conditions internal air temperature of the greenhouse was reduced to  $32.4$ ,  $30.1^\circ\text{C}$ . and in the

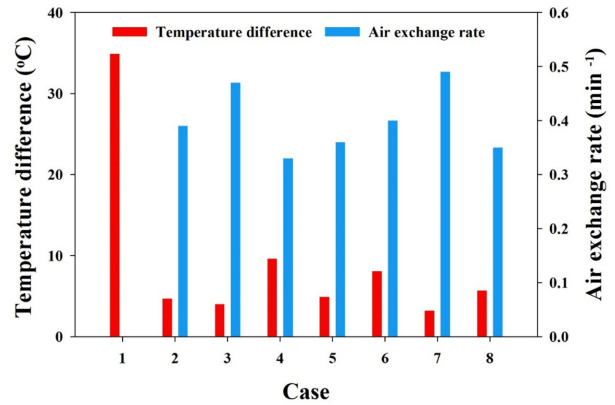


Fig. 8. Air exchange rate and inside-to-outside air temperature difference of the greenhouse for all studied cases.

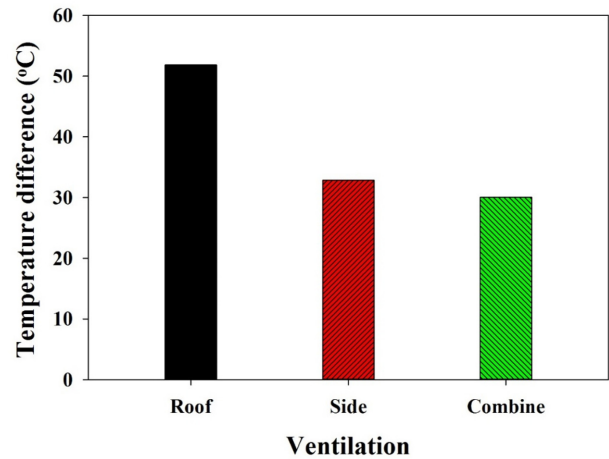


Fig. 9. Internal air temperature of the gothic-shaped conical type roof vent with different vent opening configurations.

only roof-vent opening greenhouse internal air temperature was very high  $50^\circ\text{C}$  (less reduction in internal air temperature) comparing other configurations. From the results obtained, we concluded that side vents contributed more to the natural ventilation of single-span greenhouse, and the combined roof- and side-vent openings achieved the highest reduction in the air temperature.

### Conclusion

The influence of buoyancy-driven natural ventilation of single-span greenhouses with different commonly used roof vent types were numerically investigated by using computational the fluid dynamic (CFD) code.

The numerical model was first successfully validated against the experimental data. Further, the efficiencies of the different greenhouse roof vents types were assessed by observing the reduction in the internal air temperature and ventilation rate. Our results showed that, for all the cases studied in this study, the gothic-shaped greenhouse with a conical type roof vent combination with side vents is the best as it achieved the lowest air temperature of 30.05°C and highest air exchange rate (0.49min<sup>-1</sup>). The results presented in this paper are from specific cases with the particular boundary conditions. Therefore, different results can be obtained in other cases and boundary conditions.

### Acknowledgements

This work was supported by the Korea Institute of Planning and Evaluation for Technology in Food, Agriculture, Forestry and Fisheries (IPET) through the Agriculture, Food and Rural Affairs Research Center Support Program funded by the Ministry of Agriculture, Food and Rural Affairs (MAFRA) (717001-7).

### Literature Cited

- Baeza, E.J., J.J. Pérez-Parra, J.I. Montero, B.J. Bailey, J.C. López and J.C. Gázquez. 2009. Analysis of the role of side-wall vents on buoyancy-driven natural ventilation in parral-type greenhouses with and without insect screens using computational fluid dynamics. *Biosystems Engineering*. 104(1): 86-96.
- Bartzanas, T., T. Boulard and C. Kittas. 2004. Effect of vent arrangement on windward ventilation of a tunnel greenhouse. *Biosystems Engineering*. 88(4): 479-490.
- Bartzanas, T., M. Kacira, H. Zhu, S. Karmakar, E. Tamimi, N. Katsoulas, I.B. Lee and C. Kittas. 2013. Computational fluid dynamics applications to improve crop production systems. *Computers Electronics in Agriculture*. 93: 151-167.
- Benni, S., P. Tassinari, F. Bonora, A. Barbaresi, D.J.E. Torreggiani and Buildings. 2016. Efficacy of greenhouse natural ventilation: Environmental monitoring and cfd simulations of a study case. 125: 276-286.
- Bournet, P., S.O. Khaoua and T. Boulard. 2007. Numerical prediction of the effect of vent arrangements on the ventilation and energy transfer in a multi-span glasshouse using a bi-band radiation model. *Biosystems Engineering*. 98(2): 224-234.
- Campan, J. and G. Bot. 2003. Determination of greenhouse-specific aspects of ventilation using three-dimensional computational fluid dynamics. *Biosystems Engineering*. 84(1): 69-77.
- Fatnassi, H., T. Boulard, C. Poncet and M. Chave. 2006. Optimisation of greenhouse insect screening with computational fluid dynamics. *Biosystems Engineering*. 93(3): 301-312.
- Haxaire, R., T. Boulard and M. Mermier. 2000. Greenhouse natural ventilation by wind forces. International Society for Horticultural Science (ISHS), Leuven, Belgium, 31-40.
- Hong, S.-W., V. Exadaktylos, I.-B. Lee, T. Amon, A. Youssef, T. Norton and D. Berckmans. 2017. Validation of an open source cfd code to simulate natural ventilation for agricultural buildings. *Computers Electronics in Agriculture*. 138: 80-91.
- Jung-Soo, H., L. In-Bok, K. Kyeong-Seok and H. Tae-Hwan. 2014. Analysis on internal airflow of a naturally ventilated greenhouse using wind tunnel and piv for cfd validation. *Protected Horticulture and Plant Factory*. 23(4): 391-400.
- Kacira, M., S. Sase and L. Okushima. 2004a. Effects of side vents and span numbers on wind-induced natural ventilation of a gothic multi-span greenhouse. *Japan Agricultural Research Quarterly: JARQ*. 38(4): 227-233.
- Kacira, M., S. Sase and L. Okushima. 2004b. Optimization of vent configuration by evaluating greenhouse and plant canopy ventilation rates under wind-induced ventilation. *Transactions of the ASAE*. 47(6): 2059.
- Lee, I.-B. and T.J.T.O.T.A. Short. 2001. Verification of computational fluid dynamic temperature simulations in a full-scale naturally ventilated greenhouse. *Transactions of the ASAE*. 44(1): 119-127.
- Lee, I.-B. and Short. 2000. Two-dimensional numerical simulation of natural ventilation in a multi-span greenhouse. *Transactions of the ASAE*. 43(3): 757.
- Lee, S.-Y., I.-B. Lee and R.-W. Kim. 2018. Evaluation of wind-driven natural ventilation of single-span greenhouses built on reclaimed coastal land. *Biosystems Engineering*. 171: 120-142.
- López, A., D.L. Valera and F. Molina-Aiz. 2011. Sonic anemometry to measure natural ventilation in greenhouses. *Sensors*. 11(10): 9820-9838.
- Mistriotis, A., G.P.A. Bot, P. Picuno and G. Scarascia-Mugnozza. 1997. Analysis of the efficiency of greenhouse ventilation using computational fluid dynamics. *Agricultural and Forest Meteorology*. 85(3): 217-228.
- Pontikakos, C., K.P. Ferentinos, T.A. Tsiligridis and A.B. Sideridis. 2006. Natural ventilation efficiency in a twin-span greenhouse using 3d computational fluid dynamics. *Proceedings of the 3rd*, Athens, Greece.
- Rasheed, A., J. Lee and H. Lee. 2018. Development and optimization of a building energy simulation model to study the effect of greenhouse design parameters. *Energies*. 11(8): 1-19.
- Senhaji, A., M. Mouqallid and H. Majdoubi. 2019. Cfd



assisted study of multi-chapels greenhouse vents openings effect on inside airflow circulation and microclimate patterns. *Open Journal of Fluid Dynamics*. 9(2): 21.  
Shklyar, A. and A. Arbel. 2004. Numerical model of the three-dimensional isothermal flow patterns and mass fluxes in a pitched-roof greenhouse. *Journal of Wind Engineering and*

*Industrial Aerodynamics*. 92(12): 1039-1059.  
Tong, G., D. Christopher and B. Li. 2009. Numerical modeling of temperature variations in a chinese solar greenhouse. *Computers Electronics in Agriculture*. 68(1): 129-139.

## 플라스틱 단동온실의 천창 종류에 따른 자연환기 효과

라쉬드아드난<sup>1</sup> · 이종원<sup>2</sup> · 김현태<sup>5</sup> · 이현우<sup>1,3,4\*</sup>

<sup>1</sup>경북대학교 농업토목공학과, <sup>2</sup>한국농수산대학 원예환경시스템학과, <sup>3</sup>경북대학교 농업과학기술연구소, <sup>4</sup>경북대학교 스마트농업혁신센터, <sup>5</sup>경상대학교 생물산업기계공학과

**적 요.** 여름철에 자연환기는 온실의 온도를 낮추는데 중요한 역할을 한다. 온실의 형태, 환기창 종류, 환기창의 위치 등은 자연환기 성능에 큰 영향을 미친다. 본 연구에서는 전산유체역학(CFD)을 이용하여 다양한 천창 구조에 대하여 측창에 따른 부력환기 효과를 비교분석 하였다. Boussinesq 가정을 사용하여 전체 계산영역에 대한 부력효과를 시뮬레이션 하였다. 또한 RNG K-ε 난류모델을 사용하였다. 일사량 효과를 시뮬레이션 하기 위해 Solar ray tracing과 함께 Discrete originates (DO) radiation 모델을 사용하였다. 실험온실 내부의 온도를 측정하여 CFD모델을 검증하였으며, 실험값과 계산값이 잘 일치하는 것으로 나타났다. 7가지의 천창구조에 대하여 온실의 내외부 온도차이와 환기횟수를 비교하였다. 내외부온도의 차이는 3.2~9.6°C 범위로 나타났고, 환기횟수는 0.33~0.49min<sup>-1</sup> 범위로 나타났다. 고갈형 천창구조 온실의 경우 내외부 온도차이가 3.2°C로 가장 낮았고 환기횟수도 0.49min<sup>-1</sup>로 가장 높게 나타나 환기효과가 가장 우수한 것으로 나타났다.

**추가 주제어:** 공기유동, 온실냉방, 온실 열환경, 전산유체역학